6-14-2018

Microgel Core/Shell Architectures as Targeted Agents for Fibrinolysis

Purva Kodlekere
Georgia Institute of Technology, purvagk@gmail.com

L. Andrew Lyon
Chapman University, lyon@chapman.edu

Recommended Citation
P. Kodlekere and A. Lyon, *Biomater. Sci.*, 2018, DOI: 10.1039/C8BM00119G.

Microgel Core/Shell Architectures as Targeted Agents for Fibrinolysis

Biomaterials Science

Accepted Manuscript

This article can be cited before page numbers have been issued, to do this please use: P. Kodlekere and A. Lyon, *Biomater. Sci.*, 2018, DOI: 10.1039/C8BM00119G.

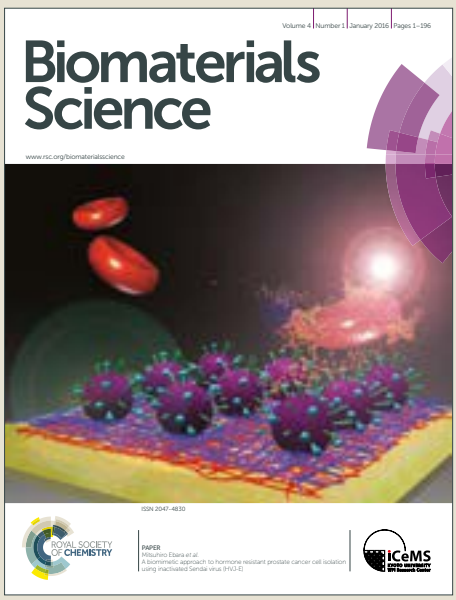

ROYAL SOCIETY OF CHEMISTRY

rsc.li/biomaterials-science

View Article Online
DOI: 10.1039/C8BM00119G

Journal Name

COMMUNICATION

Microgel Core/Shell Architectures as Targeted Agents for Fibrinolysis†

Received 00th January 20xx,
Accepted 00th January 20xx

DOI: 10.1039/x0xx00000x

www.rsc.org/

Purva Kodlekere,*[a,§] L. Andrew Lyon*[a,b]

We demonstrate the utility of microgel core/shell structures conjugated to fibrin-specific peptides as fibrinolytic agents. Poly(*N*-isopropylmethacrylamide) (pNIPMAm) based microgels conjugated to the peptide GPRPFPAC (GPRP) were observed to bring about fibrin clot erosion, merely through exploitation of the dynamic nature of the clots. These results suggest the potential utility of peptide-microgel hybrids in clot disruption and clotting modulation.

Fibrin is a biopolymer that plays a vital role in hemostasis. In the occurrence of an injury, fibrinogen, its soluble precursor, is enzymatically converted to insoluble fibrin.[1] A delicate balance between the formation of fibrin clots and their dissolution is critical for maintaining normal bodily function. Dissolution of clots in the body is carried out by the fibrinolytic system, which primarily functions *via* the action of plasmin, through activation of its precursor plasminogen. The presence of abnormal clots or thrombi leads to physiological states such as deep vein thrombosis, atherosclerosis and strokes. In order to dissolve such thrombi, plasminogen activators are commonly used. However, direct intravenous administration of these agents can cause off-target effects and lead to massive hemorrhage.[2] In order to increase the efficacy of these agents and reduce off-target effects, a number of target-specific delivery agents have been developed.[3-5]

Microgels or colloidally stable hydrogel microparticles have been utilized for the targeted delivery of therapeutics in the past. A number of these studies have involved the utilization of ligands or moieties such as proteins or peptides for targeting, while using a separate therapeutic agent that is generally encapsulated within the microgel matrix.[6-8] However, there are very few reports on the utilization of the therapeutic ability of the microgel-ligand conjugates themselves, without a supplemental therapeutic agent.[9] The elimination of variables associated with the release of a loaded therapeutic could, in principle, result in a more predictable system having a more tightly-controlled function. The interactions of colloidal particles with pre-formed fibrin clots have been studied before.[10, 11] Additionally, colloids have also been employed as imaging agents targeted to fibrin.[12, 13]

Herein, we present core/shell (C/S) microgels to be used in fibrinolysis. The grafting of the fibrin-specific peptide GPRP (fibrin knob 'A' mimic) to microgels generated conjugates that successfully disrupted fibrin clots, presumably *via* competitive binding to the holes 'a' in fibrin. These results are promising because this system exploits the nature of fibrin as an equilibrium polymer[14] in order to cause clot disruption. The occurrence of this disruption in the presence of micromolar concentrations of targeting peptide, in the absence of an external fibrinolytic agent, demonstrates the novelty and potential utility of this system.

Particles in three size ranges were synthesized to analyze the influence of microgel size on their interactions with fibrin clots. We hypothesized that the porosity of fibrin clots would lead to differences in particle residence time. The microgels were synthesized to have shells with carboxylic acid functionalities that later facilitated conjugation of the fibrin-specific peptides to the microgels.

C/S microgels were synthesized using a seed-and-feed approach[15] (Scheme S1, ESI). The synthesis conditions for small (S C/S), intermediate (I C/S), and large (L C/S) particles are shown in Table 1. Their pH responsivity, sizes and polydispersities were analyzed *via* Dynamic Light Scattering, and their spherical profiles were examined by Atomic Force Microscopy (Fig. S1 and S2, ESI). Rhodamine was incorporated in a polymerizable form (methacryloxyethyl thiocarbamoyl rhodamine B, mRhoB) while synthesizing the cores, to aid microgel visualization in flow experiments.

[a] *School of Chemistry and Biochemistry, Georgia Institute of Technology, Atlanta, Georgia 30332, USA.*
[b] *Schmid College of Science and Technology, Chapman University, Orange, California 92866, USA.*
[§] Present address: DWI Leibniz Institute for Interactive Materials e.V., D-52056 Aachen, Germany.
†Electronic Supplementary Information (ESI) available: Experimental methods, microgel characterization, encapsulation studies and a movie demonstrating clot disruption. See DOI: 10.1039/x0xx00000x

View Article Online
DOI: 10.1039/C8BM00119G

Journal Name

COMMUNICATION

Table 1. Synthesis conditions for small, intermediate and large Core and C/S microgels

Microgel type		Volume of core solution (mL)	[NIPMAm] (mol%)	[BIS] (mol%)	[mRhoB] (mM)	[AAc] (mol%)	[SDS] (mM)	[APS] (mM)	R_H (nm) at pH 7*
S C/S	Core[α]	-	98	2	0.1	-	8	8	-
	C/S[β]	10	93	2	-	5	2	0.5	102±3
I C/S	Core[α]	-	98	2	0.1	-	2	2	-
	C/S[β]	10	93	2	-	5	2	0.5	391±18
L C/S	Core[α]	-	98	2	0.1	-	0.5	0.5	-
	C/S[β]	10	93	2	-	5	2	0.5	591±39

[α][Total monomer] = 140 mM
[β][Total monomer] = 50 mM
Temperature = 70 °C
*Measurements in phosphate buffer (50 mM ionic strength)

The development of an effective, microgel-based system for targeted delivery of thrombolytic agents to fibrin clots requires an investigation into microgel localization in and around clots. This is essential to determine the efficacy of microgels for the purpose of fibrinolysis, because the rate of clot degradation will depend on the region in the clot from where it commences, and on the manner of its progression. The interplay between microgel size and fibrin clot porosity is thus crucial, particularly because microgels are deformable and hence can undergo more intricate interactions with the clots than comparable hard sphere colloids.[9, 16]

The porosity of a fibrin clot depends on the clot formation conditions.[17-19] In this study, the concentration of fibrinogen used for clot formation was 3 mg/mL, which is close to the physiological range of ~2.5 mg/mL; the clots were made using 1 U/mL thrombin.

Scheme 1 represents the experimental set up for the flow studies. In a typical experiment, the permeability of fibrin clots was first analyzed using Darcy's law, which relates the average interstitial fluid velocity to permeability of the medium. The average value of Darcy's constant 'k', i.e. permeability, for all clots used in three trials of the experiment was found to be $(4.027 \pm 0.389) \times 10^{-13}$ m^2, which is in the same range as values obtained for similarly prepared fibrin clots in previous studies.[11, 20]

View Article Online
DOI: 10.1039/C8BM00119G

Journal Name

COMMUNICATION

Scheme 1. Experimental setup used for examination of perfusion through fibrin clots

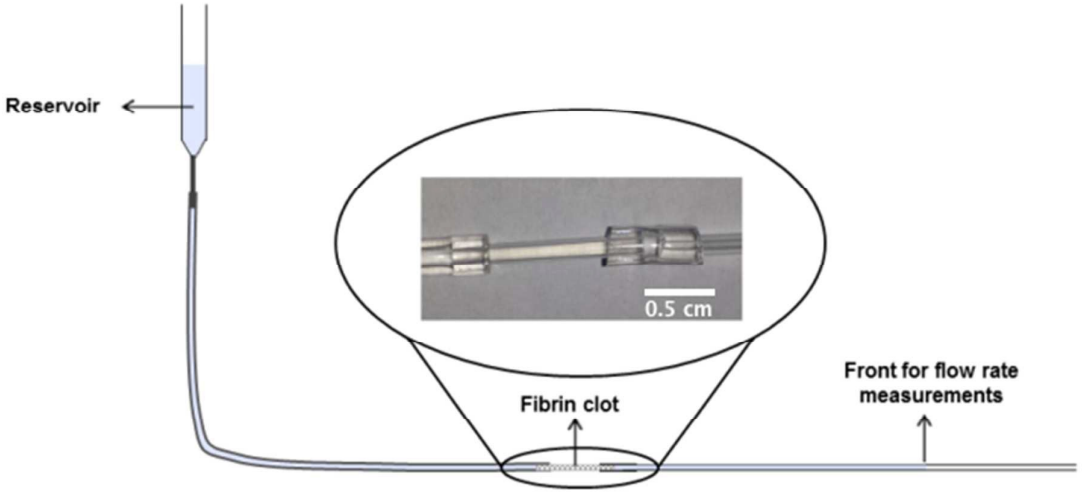

ions.
1.

In every trial, once uniformity in permeabilities was ensured, microgel solutions were allowed to flow through the respective clots. Following equilibration, eluents were collected at 30 min intervals (60 min, if necessary for collection of sufficient eluent for analysis), and were analyzed based on the fluorescence of mRhoB at λ_{ex} = 540 nm and λ_{em} = 575 nm. All fluorescence values were normalized to those of the

View Article Online
DOI: 10.1039/C8BM00119G

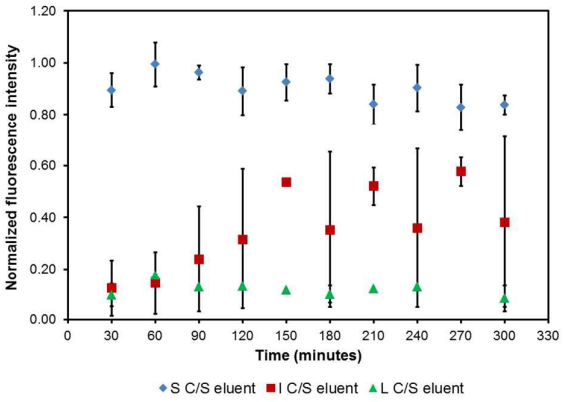

Figure 1. Eluents collected at specific time points following flow of microgel solutions through fibrin clots demonstrated differential microgel-clot interactions based on microgel size. Minimal, strong and no interactions were shown by S C/S, I C/S and L C/S microgels, respectively, owing to their size relative to clot porosity.

The flow studies revealed differences in microgel passage and residence within fibrin clots based on microgel dimensions. S C/S microgels were observed to pass through the clots easily, appearing in the eluent almost immediately. This suggests that these particles had minimal interactions with the clot, possibly due to their diameters being significantly smaller than the average pore size of the clot. I C/S microgels traversed through the clot slower than the S C/S microgels, appearing in the eluent only beyond the 1 h time point and in seemingly smaller numbers. This suggests that their dimensions may be in the range of the average pore size of fibrin clots formed under the aforementioned conditions. Thus, I C/S microgels appear to interact strongly with clot fibers. L C/S microgels were unable to penetrate the clot and did not appear in the eluent in the 5 h time frame of the experiment. Instead, these microgels concentrated at the front interface of the clot, forming a macroscopically visible boundary (visualized *via* the color of mRhoB). Conjugates of these microgels with fibrin-specific ligands could constitute a toolbox for targeting clots of different architectures. S C/S microgels could be utilized for facilitating fibrinolysis of dense clots with small pore sizes, due to their ability to target the interior regions of such clots. L C/S microgels on the other hand, would be better suited for initiating fibrinolysis at the surfaces of such clots, or in the internal regions of clots with larger pore sizes.

Keeping the above results in mind, fibrin specificity was imparted to the L C/S microgels by conjugating peptide mimics of fibrin knobs 'A' and 'B' with amino acid sequences GPRPFPAC (GPRP) and AHRPYAAC (AHRP), respectively. During the polymerization of fibrinogen, the fibrinopeptides in the center of the molecule are cleaved by the proteolytic action of thrombin. This leads to the generation of 'free' knobs 'A' and 'B', which specifically interact with the holes 'a' and 'b' present at the ends of the fibrinogen molecules, eventually forming fibrin.[1] Exposed holes 'a' and 'b' are present in the fibrin structure even after polymerization. Their presence, and the specific A:a and B:b knob:hole interactions have been exploited in this study. The aforementioned peptide mimics and other similar sequences have been studied for their fibrin specificity in the past.[21, 22] A control peptide GPSP (GPSPFPAC) was also microgel conjugated to investigate the impact of a non-binding peptide. This led to the generation of L C/S-GPRP, L C/S-GPSP and L C/S-AHRP conjugates. The purified microgel-peptide conjugates were then used in a flow study set up similar to the one represented in Scheme 1.

The flow studies were performed with fibrin clots made using 2 mg/mL fibrinogen and 1 U/mL thrombin. Prior to administering the flow of microgel-peptide conjugates through the clots, permeability studies were conducted on the clots to ensure uniformity. The Darcy constants for trials 1 and 2 represented in Fig. 2 were calculated to be $(6.3 \pm 0.18) \times 10^{-13}$ m^2 and $(8.17 \pm 0.30) \times 10^{-13}$ m^2, respectively. Following this, the buffer in the reservoirs was replaced with solutions of L C/S, L C/S-GPRP, L C/S-GPSP and L C/S-AHRP microgels, all at concentrations of 0.1 mg/mL. The clots were allowed to equilibrate for 10 min, after which flow rates of the microgel solutions through the clots were measured at 10 min intervals. The results of these measurements are presented in Fig. 2.

View Article Online
DOI: 10.1039/C8BM00119G

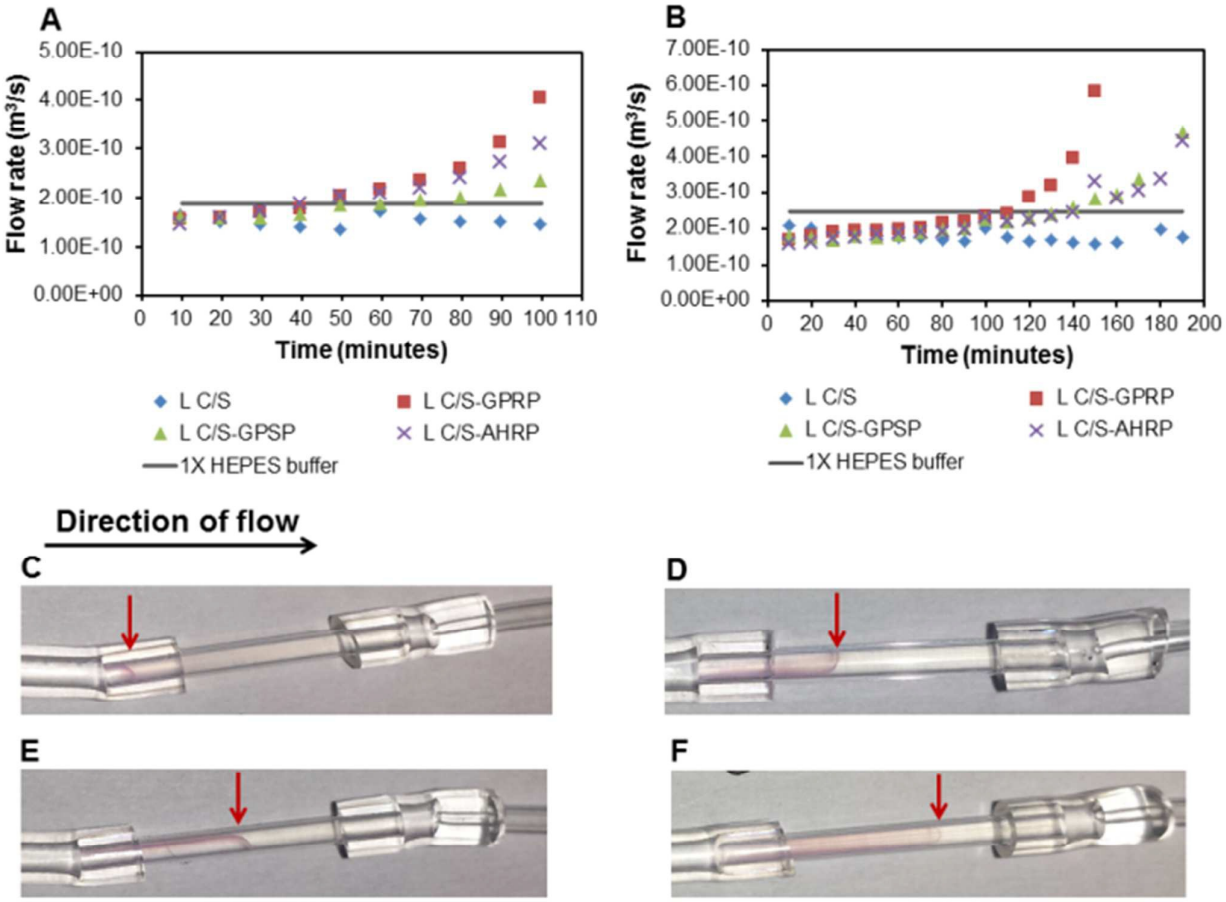

Figure 2. Trial 1 (A) and trial 2 (B) for flow rate measurements of microgel solutions through fibrin clots. Gray lines indicate flow rate of 1X HEPES buffer through the fibrin clots. Pictures of clots after passage of L C/S (C), L C/S-GPSP (D), L C/S-AHRP (E) and L C/S-GPRP (F) solutions for 100 min, taken during trial 1. Red arrows indicate extent of microgel passage through clots, bringing about partial (D, E) or complete (F) clot disruption.

Flow rate measurements over time and pictures of clots taken revealed an initial gradual increase in the flow rates of the solutions, followed by the complete disruption of fibrin

View Article Online
DOI: 10.1039/C8BM00119G

clots by L C/S-GPRP microgels over the course of the experiment (Fig. 2A, B, F). The commencement of disruption is at the time point where the increase in flow rate is appreciably higher than that of passage of HEPES buffer through the fibrin clot. Beyond this point, there is a dramatic increase in flow rate signaling complete clot disruption. This progression can also be observed in Supplementary Movie M1, obtained through a time lapse recording. Additionally, it can be followed *via* a decrease in the size of the clot, from 1.50 cm at the beginning of the experiment to 1.32 cm, 1.20 cm, 1.05 cm, 0.85 cm and 0.53 cm corresponding to the 20 min, 40 min, 60 min, 80 min and 100 min time points respectively. Fig. 2C demonstrates the integrity of the fibrin clot subsequent to flow of the L C/S microgel solution through it. This can also be witnessed quantitatively *via* the consistent values of flow rate (Fig. 2A, B). These observations allow the elimination of shear stress as a factor involved in the clot disruption. Therefore, the fibrinolysis can be accounted for primarily by the interactions of the L C/S-GPRP microgels with the clots, and can be explained in the following manner.

It has been assumed for some time that fibrin clot formation is irreversible and that clot disruption can occur only in the presence of the active enzyme plasmin or under non-physiological conditions. The presence of the tetrapeptide GPRP (tGPRP) and PEGylated GPRP during polymerization has been known to inhibit polymer formation through competition with the knobs 'A' for interactions with the complementary holes.[22, 23] However, after clot formation, the effect of such peptides on fibrin has only been studied briefly. In 2012, Chernysh et al. demonstrated that fibrin clots behave as equilibrium polymers.[14] They hypothesized that fibrin monomers and/or oligomers continually dissociate and associate with the formed fibers. Bale et al. observed a decrease in storage moduli of fibrin clots when 5.8 mM tGPRP solution was diffused into them, eventually leading to clot liquefaction after two days.[24] It is worthwhile to note that the clots utilized in both these studies were formed under different conditions. Nevertheless, the dissolution of the clots observed by L C/S-GPRP microgel conjugates can be attributed to similar phenomena. The presence of deformable microgels with multivalent surface display of peptides presumably increases the probability of adjacent, dissociated knob:hole junctions being simultaneously occupied by GPRP moieties on the microgels, leading to an enhanced effect. Based on the theoretical moles of AAc in the microgels, and assuming 100% efficiency of peptide conjugation, the upper limit of GPRP concentration in a microgel-peptide conjugate solution is in the micromolar range. This is at least two orders of magnitude below the free GPRP concentrations used in the aforementioned studies. Additionally, complete clot disruption is observed to take place in less than 3 h from the beginning of the flow experiment. This further suggests the importance of multivalency in the microgel approach. The difference in disruption time seen in the two trials may be explained on the basis of the sensitivity of this technique to small variations in clot permeabilities. L C/S-AHRP and L C/S-GPSP microgels are also seen to increase flow rate of solution through the clots, indicating partial clot dissolution (Fig. 2E, D respectively). Complete dissolution was not observed in either of these cases within the time period of the experiment and additional experiments need to be conducted in order to study these processes in detail over a longer time frame. However, partial dissolution may be attributed to non-specific interactions, weak AHRP:knob 'B' interactions,[21, 22] and similarity in GPRP and GPSP peptide sequences.

To summarize, we have developed C/S microgels with the potential to be used as fibrinolytic agents. Flow studies revealed size-based differential residence of these microgels in fibrin clots. Finally, we demonstrated that conjugation of knob 'A' peptide mimics to the L C/S microgels generated constructs capable of disrupting fibrin clots presumably through competition with the knobs 'A' on fibrin. This competition was for intermolecular interactions with the holes 'a', generated during equilibrium dissociation and association of monomers and/or oligomers. The multivalent display of GPRP peptides on microgels likely plays an important role in this disruption, leading to a faster rate of clot dissolution, at a lower overall concentration of peptide in the dispersion, in comparison to previous studies. These constructs thus have the ability to target and dissolve fibrin clots. Moreover, they also have the potential of being loaded with relevant imaging agents for visualization of fibrin clots, or with supplemental thrombolytic agents (proof of concept studies done with positively charged Green Fluorescent Protein, Fig. S3 and S4, ESI), with possible triggered, targeted release at the site of the clots, to facilitate an even faster rate of fibrinolysis.

Conflicts of interest

There are no conflicts to declare.

Acknowledgments

We would like to thank Prof. Thomas Barker for granting access to the Barker laboratory's tissue culture facilities at Georgia Tech, where the production and purification of +6 GFP was performed. We would also like to express our gratitude towards the members of the Barker group for providing training with the same, and additionally to Dr. Nicole Welsch and Dr. Ashley Carson Brown for their timely guidance. Lastly, we are grateful to the laboratory of Prof. David Liu (Howard Hughes Medical Institute, Harvard University), for providing the plasmids with genes encoding for +6 GFP.

Notes and references

1. J. W. Weisel, in *Advances in Protein Chemistry*, Academic Press, Editon edn., 2005, vol. Volume 70, pp. 247-299.
2. J. R. Marler, T. Brott, J. Broderick, R. Kothari, M. Odonoghue, W. Barsan, T. Tomsick, J. Spilker, R. Miller, L. Sauerbeck, J.

View Article Online
DOI: 10.1039/C8BM00119G

Jarrell, J. Kelly, T. Perkins, T. McDonald, M. Rorick, C. Hickey, J. Armitage, C. Perry, K. Thalinger, R. Rhude, J. Schill, P. S. Becker, R. S. Heath, D. Adams, R. Reed, M. Klei, S. Hughes, J. Anthony, D. Baudendistel, C. Zadicoff, M. Rymer, I. Bettinger, P. Laubinger, M. Schmerler, G. Meirose, P. Lyden, K. Rapp, T. Babcock, P. Daum, D. Persona, M. Brody, C. Jackson, S. Lewis, J. Liss, Z. Mahdavi, J. Rothrock, T. Tom, R. Zweifler, J. Dunford, J. Zivin, R. Kobayashi, J. Kunin, J. Licht, R. Rowen, D. Stein, J. Grisolia, F. Martin, E. Chaplin, N. Kaplitz, J. Nelson, A. Neuren, D. Silver, T. Chippendale, E. Diamond, M. Lobatz, D. Murphy, D. Rosenberg, T. Ruel, M. Sadoff, J. Schim, J. Schleimer, R. Atkinson, D. Wentworth, R. Cummings, R. Frink, P. Heublein, J. C. Grotta, T. Degraba, M. Fisher, A. Ramirez, S. Hanson, L. Morgenstern, C. Sills, W. Pasteur, F. Yatsu, K. Andrews, C. Villarcordova, P. Pepe, P. Bratina, L. Greenberg, S. Rozek, K. Simmons, T. G. Kwiatkowski, S. H. Horowitz, R. Libman, R. Kanner, R. Silverman, J. Lamantia, C. Mealie, R. Duarte, R. Donnarumma, M. Okola, V. Cullin, E. Mitchell, S. R. Levine, C. A. Lewandowski, G. Tokarski, N. M. Ramadan, P. Mitsias, M. Gorman, B. Zarowitz, J. Kokkinos, J. Dayno, P. Verro, C. Gymnopoulos, R. Dafer, L. Dolhaberriague, K. Sawaya, S. Daley, M. Mitchell, M. Frankel, B. Mackay, C. Barch, J. Braimah, B. Faherty, J. Macdonald, S. Sailor, A. Cook, H. Karp, B. Nguyen, J. Washington, J. Weissman, M. Williams, T. Williamson, M. Kozinn, L. Hellwick, E. C. Haley, T. P. Bleck, W. S. Cail, G. H. Lindbeck, M. A. Granner, S. S. Wolf, M. W. Gwynn, R. W. Mettetal, C. W. J. Chang, N. J. Solenski, D. G. Brock, G. F. Ford, G. L. Kongable, K. N. Parks, S. S. Wilkinson, M. K. Davis, G. L. Sheppard, D. W. Zontine, K. H. Gustin, N. M. Crowe, S. L. Massey, M. Meyer, K. Gaines, A. Payne, C. Bales, J. Malcolm, R. Barlow, M. Wilson, C. Cape, T. Bertorini, K. Misulis, W. Paulsen, D. Shepard, B. C. Tilley, K. M. A. Welch, S. C. Fagan, M. Lu, S. Patel, E. Masha, J. Verter, J. Boura, J. Main, L. Gordon, N. Maddy, T. Chociemski, J. Windham, H. S. Zadeh, W. Alves, M. F. Keller, J. R. Wenzel, N. Raman, L. Cantwell, A. Warren, K. Smith, E. Bailey, K. M. A. Welch, B. C. Tilley, J. Froehlich, J. Breed, J. D. Easton, J. F. Hallenbeck, G. Lan, J. D. Marsh and M. D. Walker, *N. Engl. J. Med.*, 1995, **333**, 1581-1587.
3. M. Q. Wang, J. X. Zhang, Z. M. Yuan, W. Z. Yang, Q. Wu and H. C. Gu, *J. Biomed. Nanotechnol.*, 2012, **8**, 624-632.
4. J. R. McCarthy, I. Y. Sazonova, S. S. Erdem, T. Hara, B. D. Thompson, P. Patel, I. Botnaru, C. P. Lin, G. L. Reed, R. Weissleder and F. A. Jaffer, *Nanomedicine*, 2012, **7**, 1017-1028.
5. S. Absar, K. Nahar, Y. M. Kwon and F. Ahsan, *Pharm. Res.*, 2013, **30**, 1663-1676.
6. E. B. Dickerson, W. H. Blackburn, M. H. Smith, L. B. Kapa, L. A. Lyon and J. F. McDonald, *BMC Cancer*, 2010, **10**.
7. M. T. Cook, S. A. Schmidt, E. Lee, W. Samprasit, P. Opanasopit and V. V. Khutoryanskiy, *J. Mat. Chem. B*, 2015, **3**, 6599-6604.
8. H. Zhang, S. Mardyani, W. C. W. Chan and E. Kumacheva, *Biomacromolecules*, 2006, **7**, 1568-1572.
9. A. C. Brown, S. E. Stabenfeldt, B. Ahn, R. T. Hannan, K. S. Dhada, E. S. Herman, V. Stefanelli, N. Guzzetta, A. Alexeev, W. A. Lam, L. A. Lyon and T. H. Barker, *Nat. Mater.*, 2014, **13**, 1108-1114.
10. M. T. Valentine, Z. E. Perlman, M. L. Gardel, J. H. Shin, P. Matsudaira, T. J. Mitchison and D. A. Weitz, *Biophys. J.*, 2004, **86**, 4004-4014.
11. R. C. Spero, R. K. Sircar, R. Schubert, R. M. Taylor, A. S. Wolberg and R. Superfine, *Biophys. J.*, 2011, **101**, 943-950.
12. D. P. Pan, M. Pramanik, A. Senpan, X. M. Yang, K. H. Song, M. J. Scott, H. Y. Zhang, P. J. Gaffney, S. A. Wickline, L. V. Wang and G. M. Lanza, *Angew. Chem.-Int. Edit.*, 2009, **48**, 4170-4173.
13. D. P. J. Pan, A. Senpan, S. D. Caruthers, T. A. Williams, M. J. Scott, P. J. Gaffney, S. A. Wickline and G. M. Lanza, *Chem. Commun.*, 2009, 3234-3236.
14. I. N. Chernysh, C. Nagaswami, P. K. Purohit and J. W. Weisel, *Sci Rep*, 2012, **2**.
15. W. H. Blackburn and L. A. Lyon, *Colloid and Polymer Science*, 2008, **286**, 563-569.
16. H. Bachman, A. C. Brown, K. C. Clarke, K. S. Dhada, A. Douglas, C. E. Hansen, E. Herman, J. S. Hyatt, P. Kodlekere, Z. Meng, S. Saxena, M. W. Spears, Jr., N. Welsch and L. A. Lyon, *Soft matter*, 2015, **11**, 2018-2028.
17. E. A. Ryan, L. F. Mockros, J. W. Weisel and L. Lorand, *Biophys. J.*, 1999, **77**, 2813-2826.
18. R. Bateman, H. Leong, T. Podor, K. Hodgson, T. Kareco and K. Walley, *Microscopy and Microanalysis*, 2005, **11**, 1018-1019.
19. H. Duong, B. Wu and B. Tawil, *Tissue Eng. Part A*, 2009, **15**, 1865-1876.
20. O. V. Kim, Z. L. Xu, E. D. Rosen and M. S. Alber, *PLoS Comput. Biol.*, 2013, **9**.
21. S. E. Stabenfeldt, J. J. Gossett and T. H. Barker, *Blood*, 2010, **116**, 1352-1359.
22. A. P. Laudano and R. F. Doolittle, *Biochemistry*, 1980, **19**, 1013-1019.
23. S. E. Stabenfeldt, N. M. Aboujamous, A. S. Soon and T. H. Barker, *Biotechnology and bioengineering*, 2011, **108**, 2424-2433.
24. M. D. Bale, M. F. Muller and J. D. Ferry, *Proc. Natl. Acad. Sci. U. S. A.*, 1985, **82**, 1410-1413.

View Article Online
DOI: 10.1039/C8BM00119G

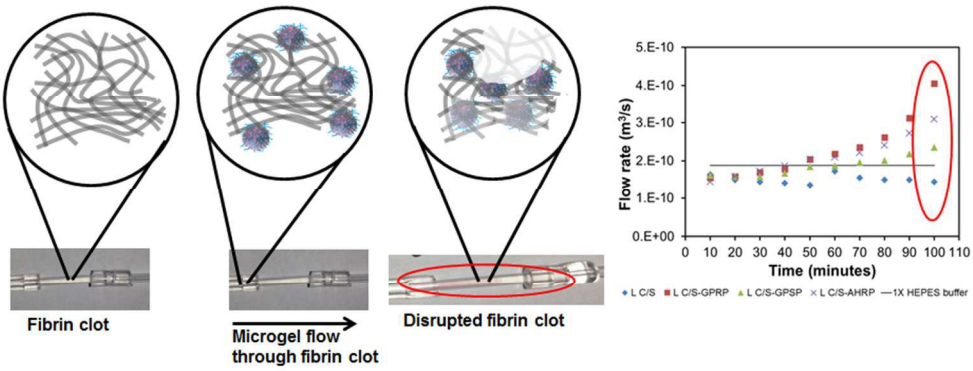

80x29mm (300 x 300 DPI)

SUPPLEMENTARY INFORMATION

for

Microgel Core/Shell Architectures as Targeted Agents for Fibrinolysis

Purva Kodlekere,*[a,§] L. Andrew Lyon*[a,b]

[a]School of Chemistry and Biochemistry, Georgia Institute of Technology, Atlanta, Georgia 30332, USA.

[b]Schmid College of Science and Technology, Chapman University, Orange, California 92866, USA.

§Present address: DWI Leibniz Institute for Interactive Materials e.V., D-52056 Aachen, Germany.

EXPERIMENTAL METHODS

Materials. All materials were purchased from Sigma-Aldrich unless specified otherwise. The primary monomer *N*-isopropylmethacrylamide (NIPMAm) was purified via recrystallization from *n*-hexane (J.T. Baker). The following were all used as received: crosslinker *N,N′*-methylenebis(acrylamide) (BIS), comonomer used for shell synthesis acrylic acid (AAc, Fluka), methacryloxyethyl thiocarbamoyl rhodamine B (mRhoB, Poly Fluor 570, Polysciences Inc.), $CaCl_2$, KCl, NaCl, anionic initiator ammonium persulfate (APS), buffer preparation materials

sodium dihydrogen phosphate, N-(2-hydroxyethyl)piperazine-N′-(2-ethanesulfonic acid) (HEPES), 4-morpholineethanesulfonic acid (MES) and formic acid (EMD Millipore), 3-aminopropyltrimethoxysilane (APTMS) for substrate functionalization for AFM imaging, coupling reagents *N*-(3-dimethylaminopropyl)-*N′*-ethylcarbodiimide hydrochloride (EDC) and *N*-hydroxysulfosuccinimide sodium salt (NHSS), 2-maleimidoethylamine trifluoroacetate salt (AEM), human fibrinogen (FIB3, Enzyme Research Laboratories), human α-thrombin (Enzyme Research Laboratories, HT 1002a), peptides from GenScript GPRPFPAC (GPRP), GPSPFPAC (GPSP) and AHRPYAAC (AHRP), ethanol, isopropanol and acetone. The solutions were prepared using distilled water, deionized to a resistance of 18 MΩ (Barnstead E-Pure system). Solutions were filtered through a 0.2 μm Acrodisc syringe filter before use.

Microgel core synthesis. Microgel cores were synthesized by free radical precipitation polymerization. In a typical synthesis, NIPMAm and BIS in molar compositions of 98% and 2% respectively were dissolved in 48.5 mL distilled, deionized water, to a total monomer concentration of 140 mM, along with SDS at the relevant concentration (refer to Table 1). The resulting solution was filtered through a 0.8 μm Acrodisc syringe filter and introduced into a 100 mL three necked, round bottom flask along with a magnetic stirrer. The flask was fitted with a thermometer, condenser and N_2 inlet and introduced into an oil bath, which was heated at 100 °C/h. Stirring was kept constant at 400 rpm and the solution was purged with N_2. Once the temperature was stable at 70 °C, 0.5 mL of a solution of mRhoB in DMSO (final concentration 0.1 mM) was introduced into the flask, following which 1 mL of the initiator APS was added after filtration through a 0.2 μm Acrodisc syringe filter. The reaction was allowed to proceed for 4 h under a N_2 blanket, after which it was cooled down to room temperature. The solution was then filtered through glass wool.

Microgel shell synthesis. Core/shell microgels were synthesized using a 'seed-and-feed' method. The shell monomer solution was prepared by dissolving NIPMAm, BIS and AAc in molar feed ratios of 93%, 2% and 5% respectively, in 39.5 mL distilled, deionized water, to a total monomer concentration of 50 mM. Following the addition of SDS (final concentration: 2 mM), the resulting solution was filtered through a 0.8 μm Acrodisc syringe filter. This monomer shell solution along with 10 mL of the respective core solution was heated to 70 °C in a manner similar to the core synthesis and was initiated with 0.5 mL APS once temperature stability was achieved. The synthesis was then allowed to proceed for 4 h under a N_2 blanket, with constant stirring at 400 rpm. It was then cooled down to room temperature and the solution was filtered through glass wool. The microgels were then purified by pelleting via ultracentrifugation at 104000–417000 × *g* for 20–70 min, depending on the microgel type. Every run of ultracentrifugation was followed by removal of the supernatant and resuspension in DI water. This process was repeated six times, after which the microgels were lyophilized prior to characterization.

Dynamic Light Scattering. Hydrodynamic radii (R_H) of the microgels were determined via dynamic light scattering (DLS, DynaPro, Protein Solutions). Measurements were performed in the following buffers: pH 7 phosphate (50 mM ionic strength), pH 7.4 HEPES (6 mM ionic strength), pH 3 formate (50 mM ionic strength) and pH 3 formate (6 mM ionic strength). Microgel samples in the respective buffers were thermally equilibrated for 20 min, following which scattering intensity fluctuations based on Brownian motion of the microgels were detected at a scattering angle of 90°. Twenty-five (25) acquisitions of 20 s each were obtained. These were used to generate intensity-time correlation functions, and cumulants analysis was used in order to

attain diffusion coefficients. The Stokes-Einstein equation was then utilized to calculate R_H values. This procedure was repeated 3 more times on the same sample in order to generate a total of 100 R_H values for each microgel sample and averages of these values along with standard deviations are presented.

Atomic Force Microscopy. Atomic Force Microscopy (AFM) was performed using an MFP-3D AFM (Asylum Research). Images were acquired in air and under ambient conditions in the tapping mode, using pyramidal cantilevers (Nanoworld, Force Constant 42 N/m) made of heavily doped silicon. Image processing was performed using software written in an IgorPro environment (Wavemetrics, Inc.)

Samples were prepared on 22 mm × 22 mm glass coverslips (VWR). The coverslips were cleaned by sequential sonication in Alconox solution, DI water, acetone, 95% ethanol, and isopropanol for 20 min each. They were then functionalized in a 1% (v/v) APTMS/absolute ethanol solution on a shaker table for 2 h, following which they were washed with DI water. The microgel solutions prepared in phosphate buffer (pH 7, 50 mM ionic strength) were then used for submonolayer deposition onto the glass substrates by centrifugation at 2250 × *g* for 10–25 min (depending on the microgel type) at 25 °C using a plate rotor. The coverslips were rinsed well with DI water and dried with nitrogen before imaging.

Production and purification of +6 GFP. Plasmids with genes encoding for +6 GFP[1] from Prof. David Liu's research group (Howard Hughes Medical Institute, Harvard University) were used for transformation of *E.coli*, following which the production and purification of the protein was performed in a manner similar to that utilized by Cronican et al.[2] with slight modifications. Briefly, transformed *E.coli* were grown to an optical density of 0.6 in LB broth

(Lennox, Alfa Aesar), following which they were induced with 1 mM IPTG (Isopropyl β-D-thiogalactopyranoside, ThermoFisher) at 30 °C for 4 h. The cells were then harvested and preserved as pellets at −80 °C. These pellets were thawed in a solution of 1X PBS with 2 M NaCl and sonication was employed to lyse them. Following centrifugation at 10000 × *g* for 8 min, the supernatant was mixed with Ni-NTA resin (Fisher Scientific) for 30 min at 4 °C. The removal of resin by centrifugation was followed by multiple washes with 2 M NaCl and 20 mM imidazole (Fisher Scientific) and then a 2 M NaCl + 500 mM imidazole solution was used for detachment of the protein from the resin. Dialysis against 1X PBS for 18 h at 4 °C was then carried out, followed by SDS-PAGE staining with Simply Blue (ThermoFisher).

+6 GFP encapsulation studies. Lyophilized core/shell microgels were weighed and resuspended in 0.20 μM +6 GFP solution in the respective buffer (6 mM ionic strength HEPES or 150 mM ionic strength HEPES). After a 20 h equilibration, the microgel solutions were centrifuged at 104000–417000 × *g* for 20–70 min, depending on the microgel type. The supernatants were analyzed for presence of +6 GFP by fluorescence measurements at λ_{ex} = 475 nm and λ_{em} = 520 nm. Normalization was performed against stock +6 GFP solutions in the respective buffer conditions.

Fibrin clot formation. Solutions of fibrinogen (13.51 mg/mL) and thrombin (10 U/mL) were thawed to room temperature. The fibrinogen was mixed with $CaCl_2$ (final concentration 5 mM), HEPES (final concentration 25 mM HEPES, 150 mM NaCl) and DI water, following which clot formation was initiated by introducing thrombin at a final concentration of 1 U/mL. The final concentration of fibrinogen was either 3 mg/mL (size-based localization studies) or 2 mg/mL (clot disruption studies). The clots were formed in plastic capillary tubes (Globe

Scientific, Inc., I.D. = 0.85 mm), and were allowed to polymerize overnight in a humid environment, to avoid abnormalities due to drying. For the perfusion experiments, they were cut into 1.5 cm pieces for utilization with each sample solution.

Permeability measurements and perfusion studies. Flow studies were performed using the experimental setup represented in Scheme 1. 1X HEPES buffer (same as that used for clot preparation) was first perfused through the 1.5 cm clots. Following 15 min equilibration, flow rates of buffer post traversal through the fibrin clots were measured for 3–5 min (depending on the clot formation conditions), from a solution reservoir height of 18 in. Three measurements were made for every clot and clot permeability values were calculated using Darcy's law,

$$Q = \frac{k}{\mu} A \frac{\Delta P}{L}$$

where Q is the volumetric flow (m^3/s), k is Darcy's constant or the Darcy permeability (m^2), μ is the liquid viscosity (kg/ms), A is the cross-sectional area of the clot (m^2), ΔP is the pressure gradient across the clot (kg/ms^2) and L is the length of the cylindrical clot (m).

Following confirmation of consistency in clot permeabilities, buffer solutions in the reservoirs were replaced by microgel solutions at a concentration of 0.1 mg/mL and these were allowed to flow through the clots. After equilibration for 15 min, eluent collection was begun and was performed at 30 min intervals. The eluents were analyzed for their fluorescence using a plate reader (Infinite® 200 PRO NanoQuant™, Tecan Group LTD., San Jose, CA) at excitation and emission wavelengths of 540 nm and 575 nm, respectively. Following background corrections for the buffer, fluorescence intensities normalized to those of the respective reservoir microgel solutions (0.1 mg/mL) were calculated. Three trials were performed and values of normalized

fluorescence intensities are presented as averages of values obtained at the respective time points from these trials. Standard deviations were also obtained from these values and are presented.

Conjugation of peptides to microgels. L C/S microgels were divided into three sections and resuspended in MES buffer (20 mM ionic strength). They were then conjugated to AEM through carbodiimide coupling, using a 2X molar excess of EDC and NHSS and a 1:1 –COOH:AEM molar ratio, based on the theoretical number of AAc moieties incorporated in the microgel shells. This conjugation was allowed to proceed for 2 h, following which dialyses for all three solutions were performed against MES buffer for 15 h. The MES buffer was then replaced with phosphate buffer (pH 7, 140 mM ionic strength) and following equilibration for ~8 h, peptide conjugations to GPRP, GPSP and AHRP (1:0.2 molar ratio of theoretical –COOH:peptide) were performed overnight through thiol-maleimide coupling. The resulting solutions were dialyzed against DI water for one week and placed on a shaker for homogeneity. A small portion of each solution was lyophilized in order to determine concentration of the stock solutions.

Clot disruption studies under flow. Clot disruption analyses were performed using a setup similar to the one utilized for permeability measurements. 1.5 cm fibrin clots were first analyzed for their consistency in permeability by conducting flow rate measurements using 1X HEPES buffer. The Darcy constant k was determined for each clot, following which reservoir buffer solutions (at an 18 in height) were replaced with the respective peptide-conjugated L C/S microgel solutions (0.1 mg/mL). After equilibration for 10 min, flow rate measurements (3 min each) were conducted for each microgel solution, after passage through the clot. This was repeated every 10 min until clot disruption was observed. Pictures of clots were also taken at

various time points during the experiment. Two separate trials were performed and the results from these are presented.

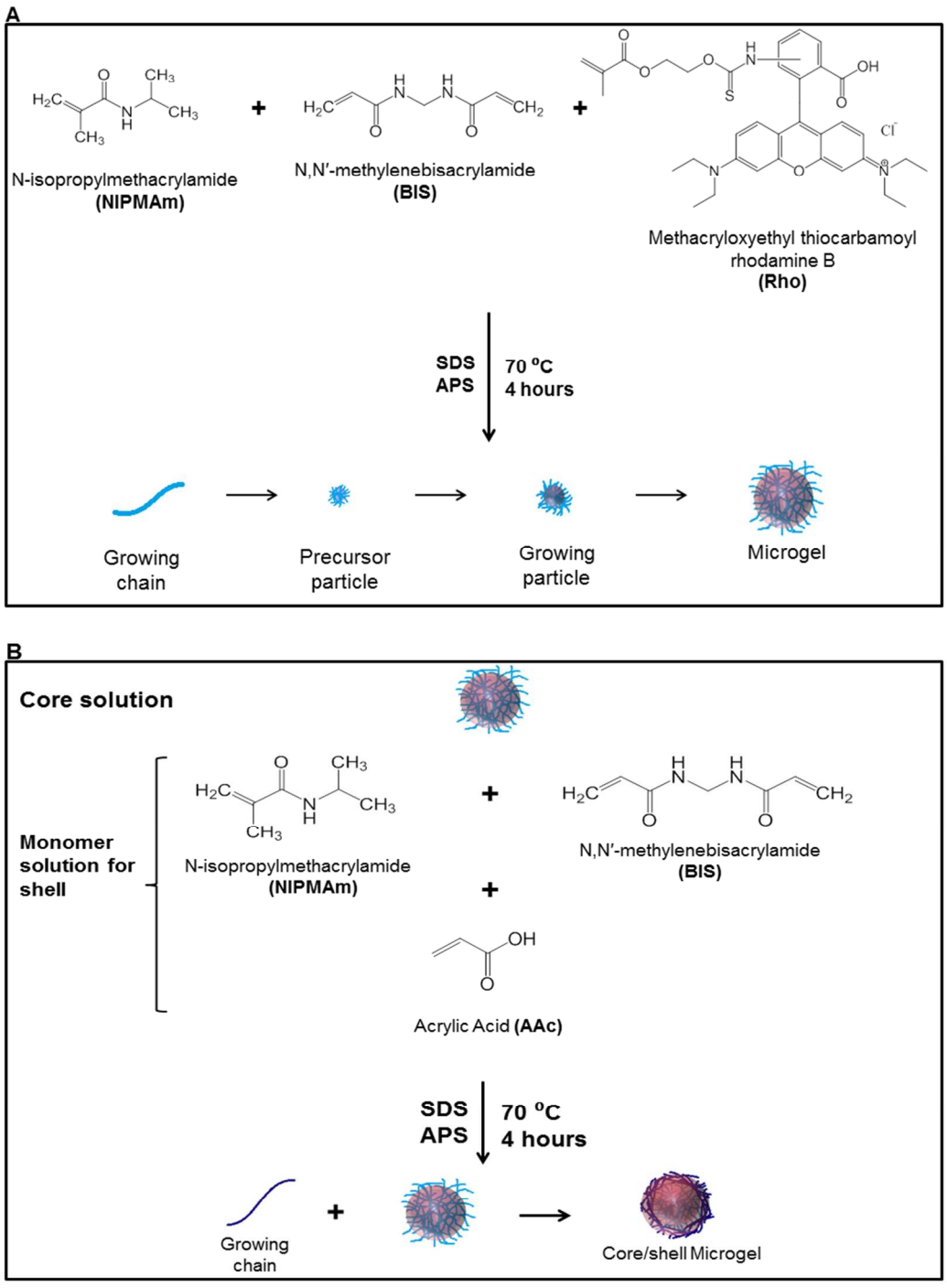

Scheme S1. General representation of a two-step core (A) and core/shell (B) microgel synthesis

Microgel characterization

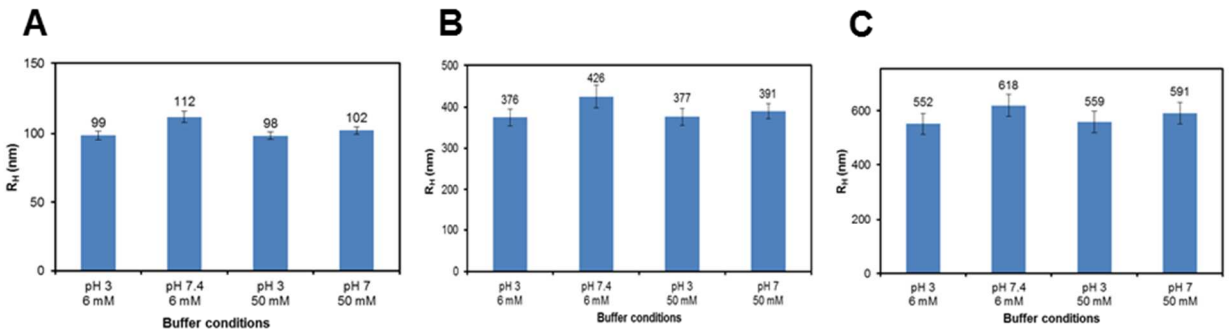

Figure S1. DLS measurements performed on S C/S (A), I C/S (B) and L C/S (C) microgels generated R_H values that demonstrated a slightly greater magnitude of pH responsivity at 6 mM ionic strength, than at 50 mM ionic strength, due to partial screening of charges in the presence of a higher concentration of ionic species in solution.

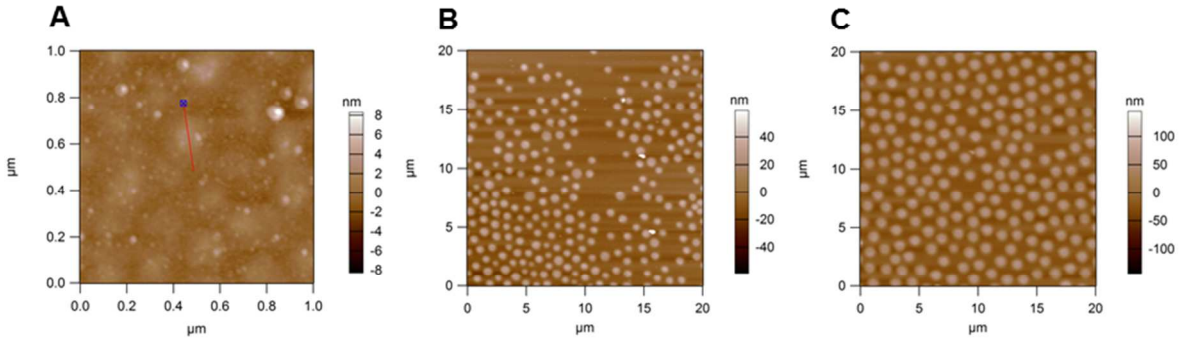

Figure S2. AFM height traces of S C/S, I C/S and L C/S microgels deposited on APTMS-functionalized glass by centrifugal deposition at 2250 × *g* for 10–25 min at 25 °C, depending on the microgel type. Particles in all three size ranges were spherical and the differences in microgel size were evident from the images and height profiles.

Production of +6 GFP

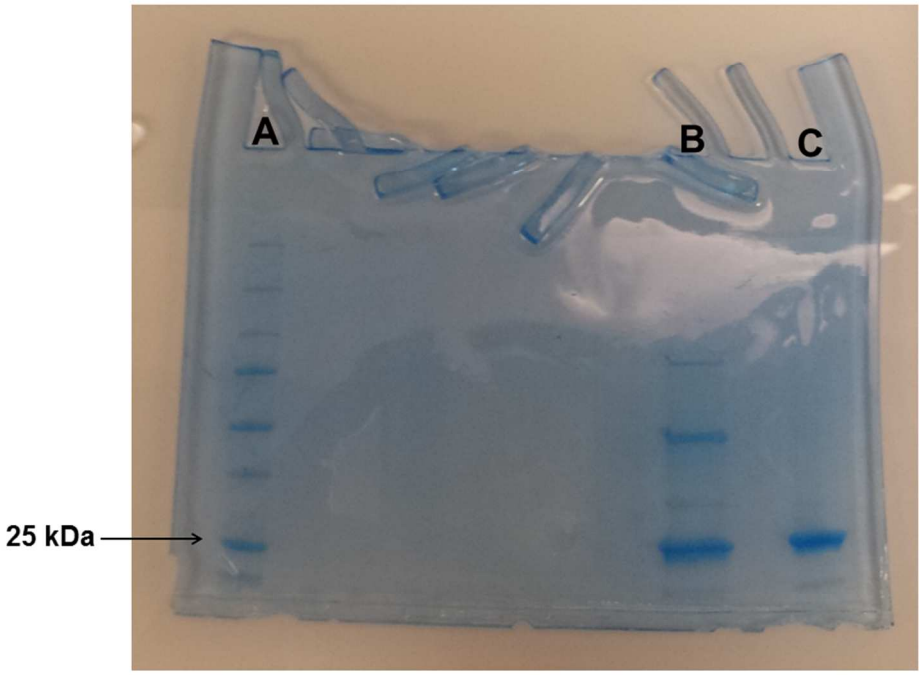

Figure S3. SDS-PAGE of purified +6 GFP. Based on the molecular weight standards (A), the bands represent the presence of +6 GFP (molecular weight of GFP is 27 kDa) [3]. B and C represent the +6 GFP solutions before and after dialysis, respectively.

Analysis of +6 GFP encapsulation in core/shell microgels

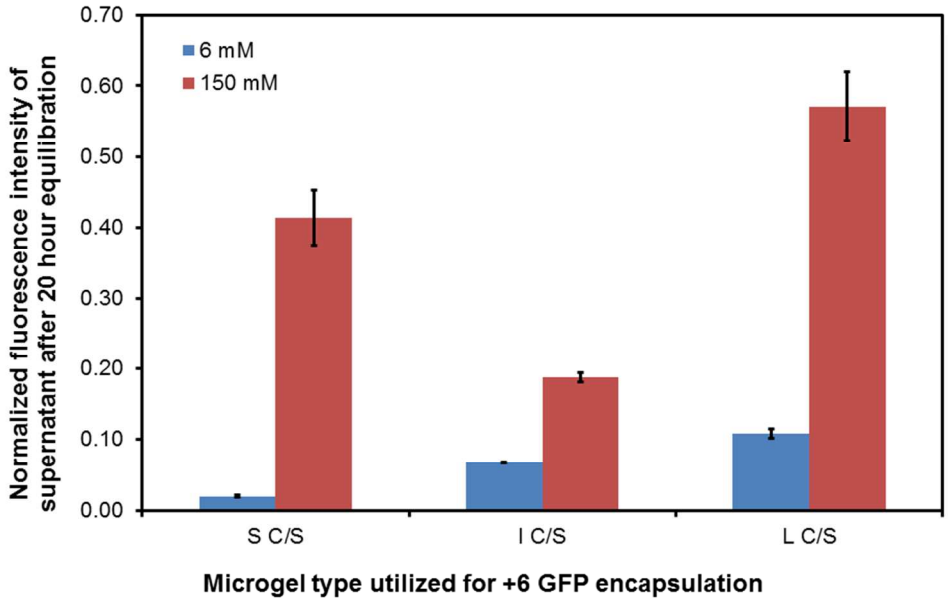

Figure S4. Analysis of encapsulation of +6 GFP by S C/C, I C/S and L C/S microgels. Fluorescence intensities of supernatants were normalized to those of +6 GFP solutions in the respective buffers. Charge screening at higher (150 mM) ionic strength was found to be effective in causing differential encapsulation *(Values presented as averages of 3 measurements on single samples, error bars represent standard deviations in these three values)*.

This analysis revealed that the size of +6 GFP (~ 27 kDa) is in a range that allows passage into microgels with the crosslinking density used in these experiments. Thus, encapsulation of other proteins with dimensions similar to +6 GFP into microgels may be feasible. Additionally, these results also indicate that charge interactions play an important role in this encapsulation.

REFERENCES

1. Lawrence, M. S.; Phillips, K. J.; Liu, D. R., Supercharging proteins can impart unusual resilience. *J. Am. Chem. Soc.* **2007**, *129* (33), 10110.

2. Cronican, J. J.; Thompson, D. B.; Beier, K. T.; McNaughton, B. R.; Cepko, C. L.; Liu, D. R., Potent Delivery of Functional Proteins into Mammalian Cells in Vitro and in Vivo Using a Supercharged Protein. *ACS Chem. Biol.* **2010**, *5* (8), 747-752.

3. Hink, M. A.; Griep, R. A.; Borst, J. W.; van Hoek, A.; Eppink, M. H. M.; Schots, A.; Visser, A., Structural dynamics of green fluorescent protein alone and fused with a single chain Fv protein. *J. Biol. Chem.* **2000**, *275* (23), 17556-17560.

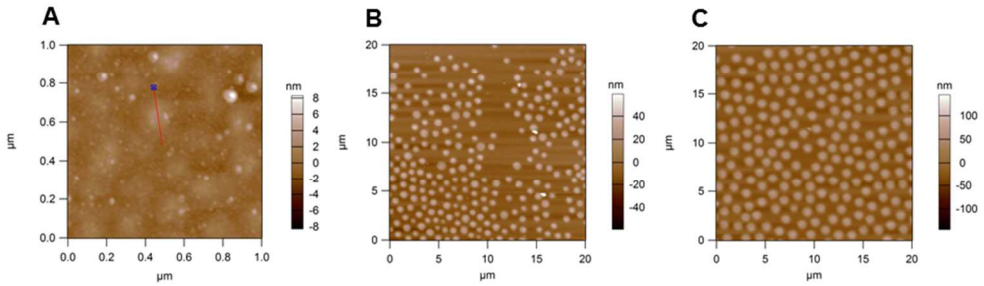

Figure S2. AFM height traces of S C/S, I C/S and L C/S microgels deposited on APTMS-functionalized glass by centrifugal deposition at 2250 × g for 10–25 min at 25 °C, depending on the microgel type. Particles in all three size ranges were spherical and the differences in microgel size were evident from the images and height profiles.

254x190mm (96 x 96 DPI)